Journal of Food Engineering 369 (2024) 111957

Contents lists available at ScienceDirect

Journal of Food Engineering

journal homepage: www.elsevier.com/locate/jfoodeng

Use of ultrasound and NIRs as tools for monitoring ice formation in superchilled meat

Silvia Grassi [a], Antonio Jiménez [b], Jorge Ruiz [c], Alberto González-Mohino [c,*]

[a] Department of Food, Environmental, and Nutritional Sciences (DeFENS), Università degli Studi di Milano, via G. Celoria 2, 20133, Milan, Italy
[b] Department of Applied Physics, School of Technology, Research Institute of Meat and Meat Product, Universidad de Extremadura, Avda de la Universidad s/n, 10003, Cáceres, Spain
[c] Department of Food Technology, Research Institute of Meat and Meat Products, Universidad de Extremadura, Avda de la Universidad s/n, 10003, Cáceres, Spain

ARTICLE INFO

Keywords:
Superchilling
Non-destructive methods
Ultrasound testing
NIR
Beef round meat

ABSTRACT

This study aimed to gain a deeper understanding of the ice crystal formation during the superchilling process (SC) of meat by using non-destructive methods. Ultrasound inspection was performed considering the ultrasonic pulse velocity (UPV), while Near Infrared Spectroscopy (NIR) measurements were carried out with a spectral range of 950–1650 nm. Signals from both methodologies were periodically taken during the controlled freezing of 8 beef cubic samples of (6 cm^3). Obtained results revealed that both methods have the ability to detect the ice crystal formation during the SC process, and particularly during the period of thermal arrest. Hence, these results evidence that ultrasound inspection and NIR, combined with Multivariate Statistical Process Control charts, could be implemented as quality control procedures during the SC process of muscle foods, allowing a more accurate control of the process and thus, minimizing the potential deleterious effects of ice crystals formation in meat.

1. Introduction

In a global scenario aiming for reducing food waste and making the whole food chain more sustainable, increasing shelf life of highly perishable foods and reducing as much as possible the energy consumption for food preservation, have become crucial strategies for food industries, and more specifically, for the meat sector (Djekic and Tomasevic, 2016). In this context, superchilling (SC) of meat, the storage at a temperature around 1-2 °C below the initial freezing point, provides a substantial extension of fresh meat shelf life of around 2–4 times as compared to regular chilling, while avoiding the disadvantages of meat freezing, such as quality deterioration and higher energy consumption (Banerjee and Maheswarappa, 2019). SC allows shipping fresh meat to distant markets and helps with the logistic of meat storage and distribution at a national level.

The common industrial setup for SC of meat involves bringing the temperature of its surface below its freezing point, either in a blast freezer or by impingement freezing, leading to the formation of an ice layer on the surface (Duun et al., 2008). Later on, during SC storage, the temperature evens out within the whole volume of meat (Banerjee and Maheswarappa, 2019). While the formation of some proportion of ice during SC is consubstantial to the process, it also directs to structural and physico-chemical changes (Pomponio et al., 2018; Pomponio and Ruiz-Carrascal, 2017), so that a higher amount of frozen water will eventually lead to a more intense damage of the muscle structure and a lower meat quality. Therefore, it results crucial to optimize the SC process, aiming for the longest possible shelf life, but also reducing as much as possible meat deterioration by controlling ice crystal formation. However, monitoring ice crystallization in meat is not an easy task, and most methods are either destructive or time consuming (Rahman, 2009). In this context, developing non-destructive rapid methods that may allow following water crystallization during SC could be very useful for industrial and research purposes.

Non-destructive ultrasonic tests allow the acoustic characterization of food samples by determining, among other parameters, the velocity of wave propagation in them (Awad et al., 2012). Ultrasound velocity has extensively been used in several food matrices and particularly in meat products for diverse objectives, for example to discriminate feeding systems (González-Mohino et al., 2022), to determine pastiness in ham (Contreras et al., 2020) and textural properties in hamburgers (Fariñas et al., 2021). In addition, it is a very sensitive parameter to temperature (Ensminger and Bond, 2011; Schmerr and Song, 2007), as has been

* Corresponding author.
E-mail address: agonzalerw@alumnox.unex.es (A. González-Mohino).

https://doi.org/10.1016/j.jfoodeng.2024.111957
Received 18 October 2023; Received in revised form 21 December 2023; Accepted 8 January 2024
Available online 9 January 2024

evidenced in pork cooking (González-Mohino et al., 2019b), in the cooling/heating process of edible oils (Jiménez et al., 2022) and in honey samples (González-Mohino et al., 2019a).

Near-infrared (NIR) spectroscopy (700–2500 nm) is a widely explored non-destructive technique for adulteration assessment concerning species (Grassi et al., 2018) processing (Alamprese et al., 2016), as well as for meat quality and safety evaluation (Sanchez et al., 2022). NIR technology versatility relies on its capability of providing multi-component description of both the physical properties and the chemical composition of food, thanks to the interaction of light with the product understudy. Furthermore, in the last decades, its usage has been incentivized due to release of miniaturized and portable NIRS instruments offering a great potential for on-site monitoring quality control along the entire meat value chain (Kademi et al., 2019). Conversely, some developed applications by NIR instruments, especially the hand-held ones, do not rely on strong scientific basis, stressing the need of physical and chemical background to support the prediction models developed in the laboratories to be then transferred to industrial conditions. The basis of NIR use for SC monitoring relies on the well-known effect of temperature on NIR signal, especially on hydrogen bond in aqueous systems (Gowen et al., 2013). Besides, its successful implementation has been proved for ice fraction prediction in SC salmon by online NIR imaging scanner measurements (Stevik et al., 2010). However, no further uses on ice formation in other food matrices, or deeper exploration of simpler instruments, such as portable NIR devices, for this purpose, have been published so far.

Thus, this study aims to gain a deeper understanding of the ice crystal formation during the SC process of meat through two non-destructive on-line methods:NIR using a portable device and ultrasonic tests.

2. Material and methods

2.1. Samples and measurement conditions

Three beef rounds were purchased from Dehesa de Solana S.A. (Cáceres, Spain). Eight cubic samples of 6 cm^3 (206 ± 11 g) were cut from the beef rounds. Table 1 reports information on the origin and weight of each of the samples analysed. Two meat cubes were obtained from beef round A for trial 2; similarly, two cubes were cut from beef round C and analysed during trial 4, whereas from round B four cubes were obtained and used in trial 1 and 3. Animals born, reared, slaughtered and deboned in Spain.

Firstly, samples were introduced in a temperature-controlled chamber (RIVACOLD RC325-45ED, Italy), and when the core of the samples reached 3.5 ± 1.0 °C, they were introduced in a freezer (SCLAB CV-20/160, Spain) with forced air ventilation at −18 °C and 0.5–0.7 m/s speed.

2.2. Trial set up

Temperature, Ultrasound and NIR measurements were performed on-line for the entire process duration (up to 330 s) by positioning the sensors as reported in Fig. 1.

The experimental setup was repeated in 4 different days allocating two cubes for each trial, one for the ultrasound measurements and one for the NIR and temperature recordings. The beef cubes were not in direct contact with ultrasound and NIR equipment, but they were covered by plastic film. An experimental design with the ultrasound and NIR measurement conditions is shown in Fig. 2.

Table 1
Origin and weight of samples monitored by ultrasound and NIR.

Round	Trial	Weight (g)
A	2- ultrasound	199.01
	2 - NIR	202.14
B	1 - ultrasound	222.61
	1 - NIR	225.02
	3 - ultrasound	201.34
	3 - NIR	191.66
C	4 - ultrasound	201.03
	4 - NIR	204.78

2.3. Temperature control

The internal cube temperature during NIRs assessments was recorded every 2 min with a T type temperature probe coupled to a temperature data logger (Testo 735–2, USA) inserted in the samples. The on-line monitoring of the temperature was not feasible for the beef cube analysed by ultrasounds, as the probe would have altered the ultrasonic signal; so, it was assumed the cubes had the same temperature along each trial.

2.4. Ultrasound analysis

Ultrasound data were collected approximately every 10 min up to 300 min. The protocols and procedures followed in the present study coincide with those reported in previous works (González-Mohino et al., 2022; Jiménez et al., 2022) with some modifications. Therefore, and due to this fact, the description is brief and emphasizing those differential aspects. The ultrasonic equipment was composed by a Panametrics-NDT Model 5077 PR pulser-receiver, which was connected to an InfiniiVision DSO-X 3032A (KEYSIGHT) oscilloscope. The beef samples were assessed using contact ultrasound methodologies with the mode of through-transmission (TT). Fig. 1 shows the set-up used for the measurements. A pair of Panametrics A114S-RB transducers (with nominal frequency of 1 MHz) was applied for the measurement. The main characteristics of A114S-RB are displayed in Table 2, showing the beam-spread angle and the near-field zone, essential to select the suitable transducers for the ultrasonic assessment (González-Mohino et al., 2022). Thus, the near field length in our tests is clearly less than the dimensions of the inspected parts, thus ensuring that all measurements were made in the far field. A coupling gel (Sonagel W) of fluid consistency was applied to the beef cube surfaces to facilitate the transmission of the waves. This gel is a non-toxic water-soluble substance with a frozen point of −15 °C, which is easy to remove. Moreover, a thin plastic covered the cubic samples to avoid the contact among gel and sample. Special care was taken to keep both transducers perfectly facing each other in the sample, using specific clamping devices that provided us at the same time the separation distance between transducers, or what is the same, the thickness of the sample (including the thickness of the transparent film), with an accuracy of ±0.01 mm.

The visualization mode chosen for the ultrasonic inspection was the A-scan. Two kinds of A-scan acquisition were captured for each sample: i) 25 μs time scale, showing trigger pulse, arrival pulse, and two first echoes, and ii) 12 μs time scale, only showing arrival pulse and first echo. These echoes are caused by the reflections of the ultrasonic waves in the opposing transducers. Both kinds of A-scan were recorded in csv files with 10 000 points. Fig. 3 displays two typical examples of each of the A-scans described. From A-scans, ultrasonic pulse velocity (UPV) was determined by means of the so-called cepstrum method (Gudra and Opielinski, 2004), which allows previously calculating the time-of-flight (TOF). Since both transducers are separated by a known distance (d), UPV is determined from Eq (1).

$$UPV = \frac{2d}{TOF}$$

2.5. NIR analysis

MicroNIR device (MicroNIR OnSite VIAVI Solutions, USA) was used to analyse one beef cubic sample for each trial by positioning the sample on the top of the measuring window. The spectra were acquired in the spectral range 950–1650 nm in diffuse reflectance every 2 min, with a

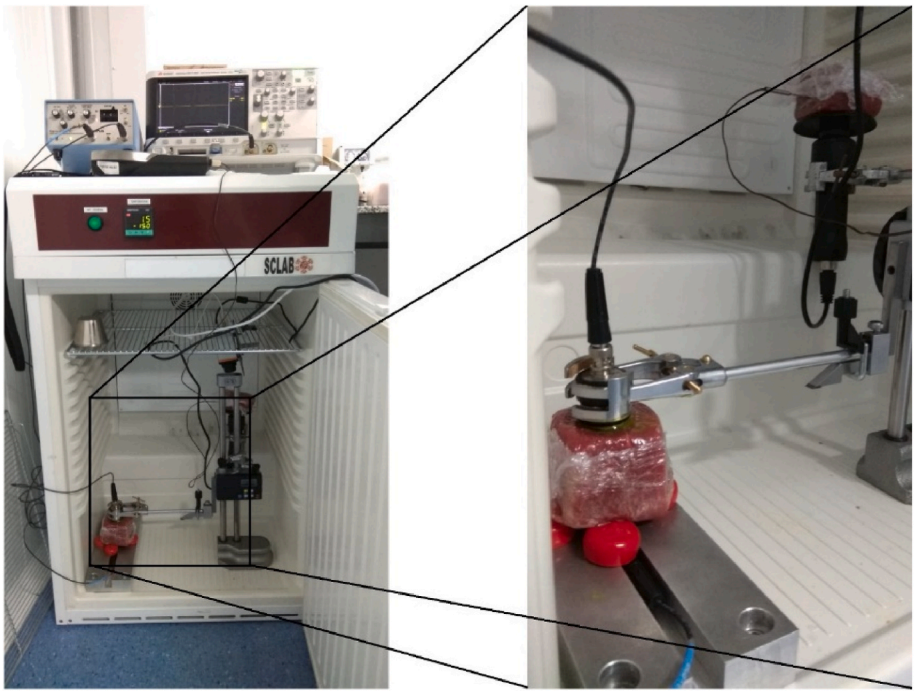

Fig. 1. Set-up used for ultrasound and NIRs measurements.

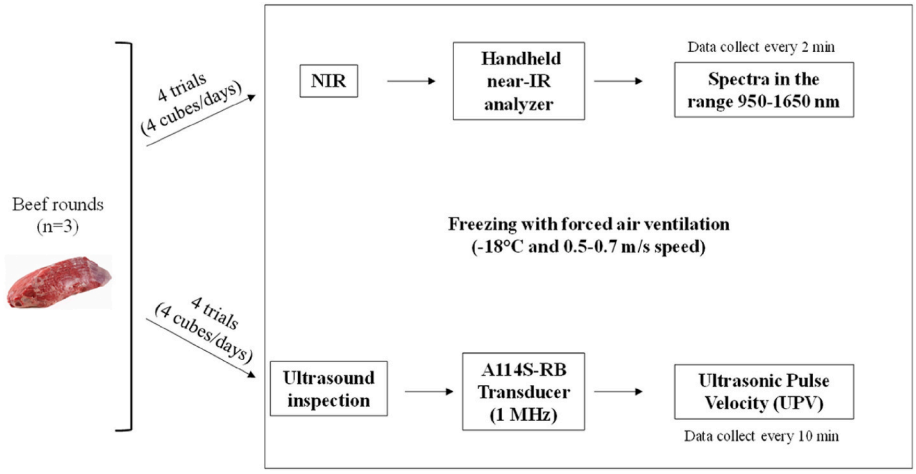

Fig. 2. Experimental design of ultrasound and NIR measurements.

Table 2
Characteristics of the transducers used.

Model	Diameter (cm)	Frequency (kHz)	Wavelength (mm)	−6 dB bandwidth (%)	N (cm)	φ (°)
Panametrics A114S-RB	1.9	1000	1.80	61.93	5.01	6.64

UPV = 1800 m/s was taken for the calculation of wavelength, N, and φ
N = near-field length.
φ = beam angle.

12.5 μs integration time and 200 scans, with a spectral bandwidth lower than 1.25% of centre wavelength, typically 1% (e.g., at 1000 nm, the resolution is lower than 12.5 nm) and signal-to-noise ratio of 25 000.

2.6. Data analysis

Ultrasound data was collected and treated by Excel software package (Microsoft, Redmond), and the plot representations were performed by software package Origin (OriginLab, Massachusetts). The data of volts and seconds from each A-scan measurement at 12 μs of the ultrasonic inspection was organized in a unique dataset, as well as the acquired NIR spectra and pretreated with different methods (Standard Normal Variate, SNV; smoothing and first derivative) and their combination. Consequently, the datasets of ultrasound data, as well as the raw spectra or pretreated ones, were explored by Principal Component Analysis (PCA). PCA is particularly useful to visualise sample distribution

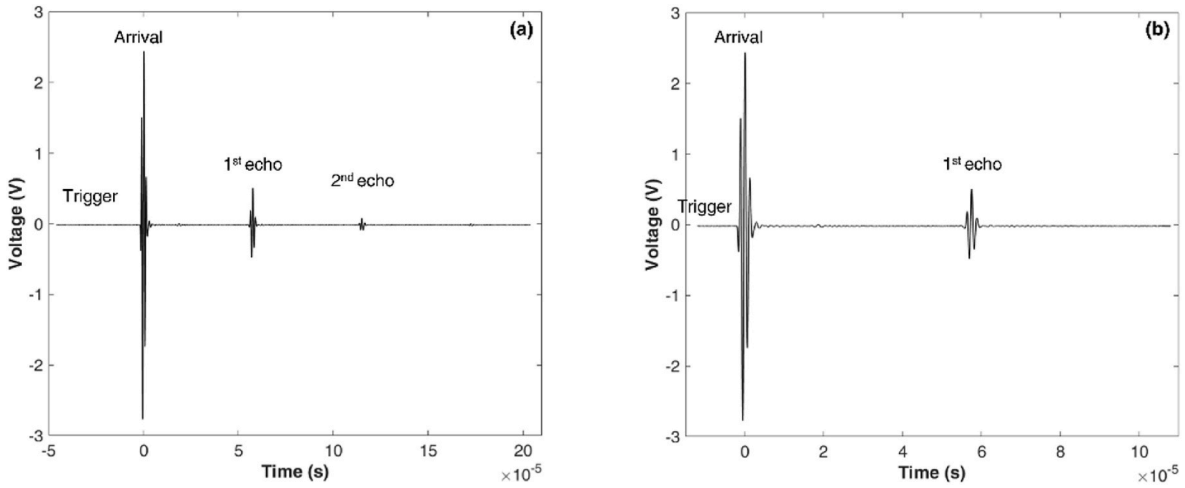

Fig. 3. Examples of A-scans obtained with the Panametrics A114S-RB transducers for piece 2: (a) 25 μs time scale and (b) 12 μs time scale.

according to the considered signal being an unsupervised exploratory procedure that allows the visualization, in a reduced space, of the relationships between objects (by the score plot) and variables (by the loading plot) (Wold et al., 1987). PCA was then used, only for the NIR spectra, to construct Multivariate Statistical Process Control (MSPC) charts for ongoing process trends description. For this application 3 out of 4 experimental trials were used to build the model (Trial 1, 2 and 4), whereas the spectra collected along trial 3 were used to validate the control chart. The PCA-based MSPC chart (MacGregor and Kourti, 1995) was developed calculating Hotelling's T^2 and Q statistics for the PCA models constructed with the MicorNIR spectra. The Hotelling's T^2 chart represents the estimated Mahalanobis distance from the centre of the PCA model, whereas the Q-statistic chart analyses the residuals, i.e., the process variations not represented in the PCA model. PCA and PCA-based MSPC chart were developed with PLS Toolbox (Eigenvector, USA) working under MATLAB environment (R2016b, The Mathworks, USA).

3. Results and discussion

3.1. Temperature profiles

Fig. 4 shows the temperature profiles during the different freezing trials. All of them show the typical freezing curve, with a period of "thermal arrest" plateau between −0.5 °C and −1.0 °C as transfer of the latent heat of freezing of water from the meat, counteracting the heat transfer from the meat to the freezer air.

This period of thermal arrest was considerably long (around 100 min), as a consequence of the freezing conditions used (−18 °C at a low air speed). These are not the common conditions for freezing or SC meat, but were more convenient for following ice crystal formation, since the formation of the ice fraction takes place more slowly, allowing the recording of measurements with small differences in temperature, and thus, in proportion of ice.

3.2. Ultrasound inspection results

Firstly, we must indicate that the amplitude of the signal corresponding to the second echo gradually decreases as the temperature of the sample inspected by ultrasound decreases, being totally imperceptible at temperatures below −0.8 °C approximately. Consequently, the cepstrum method could not be applied in the A-scans of 25 μs below the mentioned temperature to obtain the velocity values. Therefore, these measures were not considered in the present study.

Fig. 5 displays the evolution of UPV against the temperature of the

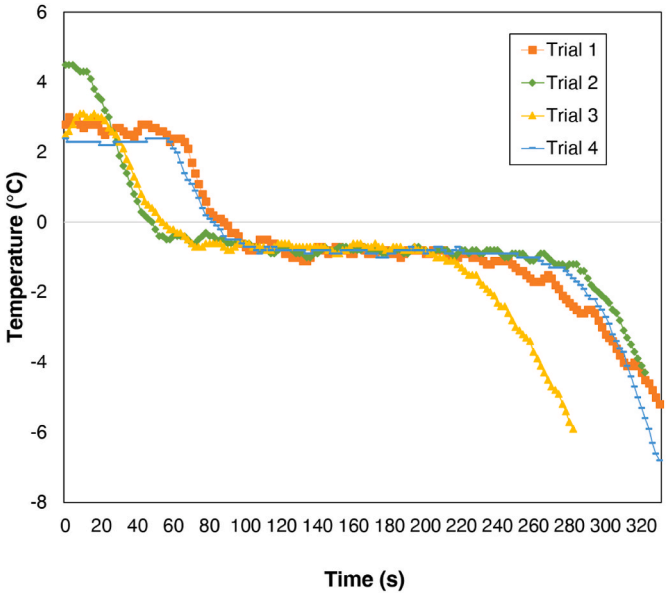

Fig. 4. Temperature profiles recorded at the core of one beef cube for each of the four trials.

four samples assessment. This behaviour closely resembles that observed in other studies involving ultrasonic monitoring of chicken breast muscle and beef round roast using 2.25 MHz transducers (Sigfusson et al., 2004). In our study, the UPV values ranged between 1508 and 1563 m/s in temperatures above 0 °C. In this way, if we consider each of the pieces individually, their velocity values are practically stable in the indicated temperature range, showing if anything a very slight increase in velocity when the temperature decreases. The results obtained were coherent with previous works in fresh meat. For beef samples, the use of low-intensity ultrasounds has scarcely been explored. Some works showed UPV values among 1575 and 1585 m/s (Diaz-Almanza et al., 2021). Abdul Halim et al. (2012) reported a range between 1200 and 1600 depending on the fat content, however this study did not consider the far-field zone. In pork loins at 7 °C, the range of UPV mean values was found among 1491 and 1550 m/s (González-Mohino et al., 2022), depending on the feeding system. Other authors determined an UPV of (1557 ± 6.3) m/s and (1534 ± 4) at 2 °C, in *Longissimus dorsi* and *Biceps femoris* samples respectively (de Prados et al., 2015). Niñoles et al. (2011), estimated the UPV at 10 °C with a range of mean values between 1580 and 1590 m/s in *Biceps femoris*. On the other hand, Nowak and

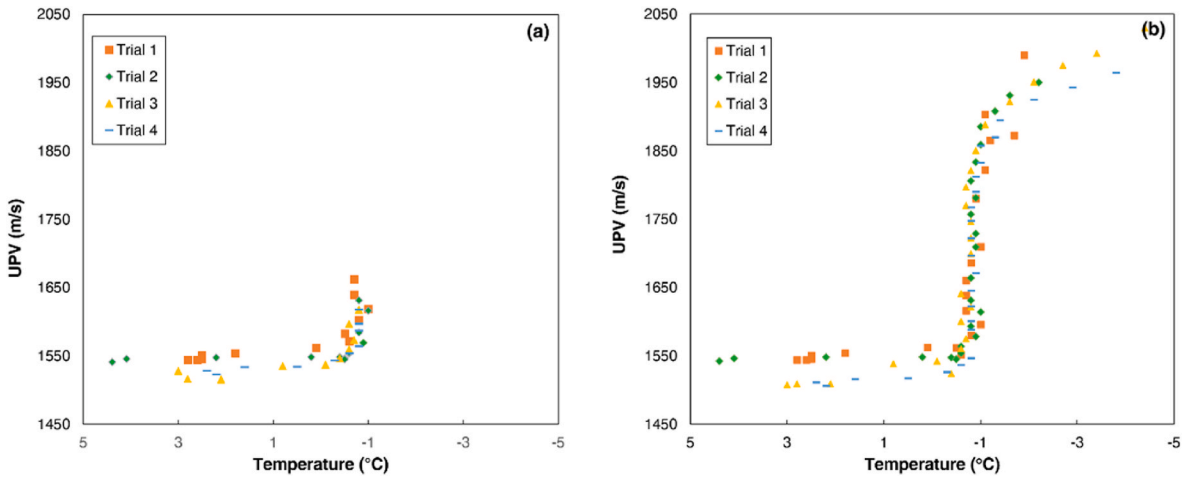

Fig. 5. Evolution of UPV with temperature for all samples: (a) 25 μs time scale and (b) 12 μs time scale.

Markowski, 2013 reported that the ultrasound velocity in pork slices was between 1552 and 1557 m/s.

Unfortunately, as the samples cooled, the second echo present in the 25 μs timescale A-scans decreased in amplitude, to the point of not being visible when the samples began to freeze. For this reason, it was impossible to calculate UPV in the 25 μs A-scans from temperatures below approximately −0.8 °C, this value varying slightly depending on the sample tested. Consequently, it was only possible to calculate UPV in all samples at all temperatures for 12 μs A-scans. Thus, in temperatures below 0 °C, and considering only the results extracted from the 12 μs A-scans (Fig. 5b), the UPV values showed a range among 1524–2030 m/s. Similarly, to the previously cited literature, higher UPV mean values were attained when the temperature decreased. This is most likely due to an increase in the stiffness of the samples as a consequence of water freezing (González-Mohino et al., 2019b). In meat products, the water content and particularly its status, exerts a high influence on UPV (Niñoles et al., 2011). However, the behaviour exhibited by the UPV in the range between −0.5 °C and −1.5 °C is striking. As can be seen, especially in the case of 12 μs A-scans, during the period of thermal arrest, in which the temperature remains stable during the freezing process, the velocity increases dramatically. It seems logical to think that this high increase in velocity is nothing more than the ultrasonic response to the mechanical changes that occur in the samples as the proportion of frozen water increases. This phase change occurred at constant temperature, producing a higher ice proportion against liquid water. As it is known, the velocity of sound propagation in ice (~3100 m/s) is significantly higher than in liquid water (~1500 m/s) (Kinsler et al., 1999). Indeed, Sigfusson et al. (2004) depict the ultrasonic velocity behaviour in water as a function of temperature, obtained with 2.25 MHz transducers, where the velocity undergoes a drastic increase from 1500 m/s at 0 °C to nearly 4000 m/s at −5 °C. Subsequently, this velocity value remains pseudoconstant for lower temperatures. Therefore, the increase of ice proportion on samples caused the increase of UPV values. Below −1.5 °C, the velocity continued increasing, although with a much gentler slope, which suggests that part of the water that remained in liquid state in the samples was still getting frozen. In this way, the velocity of propagation of ultrasonic waves seems to indicate much more accurately than the temperature itself the content of the proportion of frozen and liquid water in the sample.

The multivariate explorative analysis, a.k.a. PCA on the 12 μs US data, confirmed the evolution for UPV according to temperature. Fig. 6 reports the evolution of PC1, describing 80.90% of the total variance of the 4 different trials against temperature. As can be seen in Fig. 6a, the PC1 score values start from highly negative scores when internal temperature is positive (>0 °C), remaining almost constant up to 0 °C, then increases dramatically during the period of thermal arrest, in which the temperature remains stable during the freezing process. Finally, when decreasing below −1 °C the PC1 scores maintain positive and almost constant values. The samples positioning is influenced by changes in the US signal mainly in the arrival (around 0 s), which resulted relevant in PC1 loadings (Fig. 6b). Indeed, the position is influenced by the mechanical changes occurring as the proportion of frozen water increases.

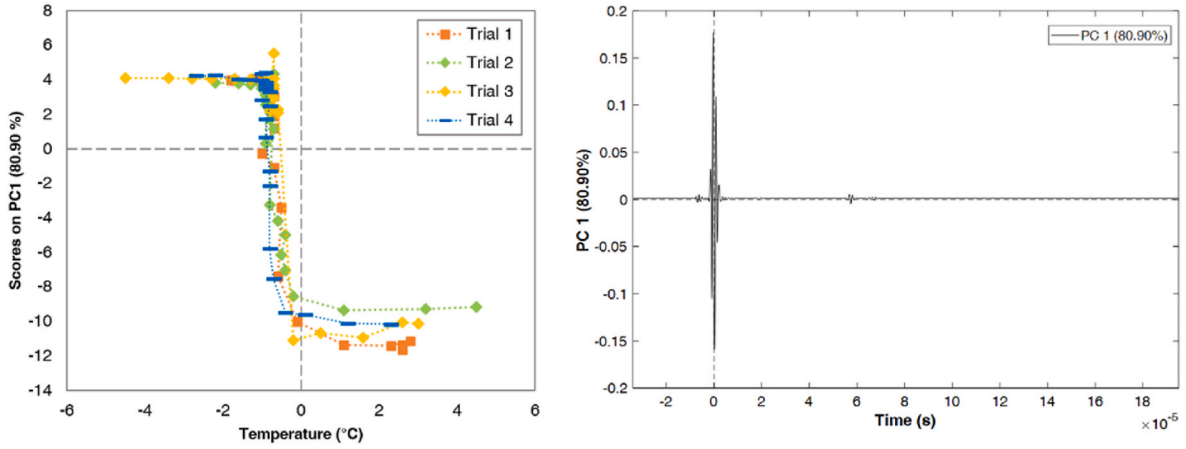

Fig. 6. Principal Component Analysis on the 12 μs time scale US data: A) PC1 scores vs internal temperature recorded for all the 4 trials; B) PC1 and PC2 loadings plot.

3.3. NIR results

The NIR spectra recorded at the beginning of the trial 4, as well as the other trials, show absorptions at 970, 1200 and 1420 nm (Fig. 7a) related to water molecule combination of symmetric stretch and bending mode, symmetric stretch, asymmetric stretch and bending mode and asymmetric stretch and bending mode, respectively (Workman and Weyer, 2008). With the decrease of temperature, a systematic shift in the water peaks was observed, i.e. a displacement of the absorption bands from 970 to 1025 nm, from 1200 to 1250 nm and from 1420 to 1500 nm (Fig. 7a) (Workman and Weyer, 2008). Similar behaviour has been observed by Stevik et al. (2010) when studying salmon fillets superchilling. They notice a shift in the water peak (from 900 to 1040) with increasing ice fraction. Moving to spectral-spatial information, the hyperspectral imaging (HSI) approach developed by the same research group confirmed the described shift in the peak maxima (Ottestad et al., 2009). Similarly, the model developed by Xie et al. (2016) to detect freezing parameters in porcine *L. dorsi* muscle assessed the relevance of absorbance at 1070, 1172, 1420, 1586, and 1890 nm on meat spectra during freezing. Not that reliable results were obtained by Cruz et al. (2023) when evaluating ice mushes by NIR, however the failure in predicting ice fraction revealed to be difficult basically due to the design of used NIR probe.

The transformation by SNV reduce the baseline shift due to light scattering and it highlighted the isosbestic points related to different stages of hydrogen-bonded water molecules (Fig. 7b and d). Signal in the range 1400–1650 nm resulted highly affected by the absorption of plastic film covering the beef cube, thus the spectral range used for further elaboration was reduced to 940–1350 nm (Fig. 7c and d).

The spectra collected along the 4 trials were merged in a unique dataset explored by PCA. To better visualise the trend, Fig. 8a reports the scores plot of trial 4, which is representative of what observable in the other trials. The scores plot of PC1 vs PC2 explained 99.85% of the total variance of the unique dataset after SNV transformation. Spectra recorded at the beginning of the monitoring, with internal temperature between 3 and 0 °C, assumes positive PC1 and negative PC2 scores. With temperature decrease it is possible to notice a fast displacement towards positive PC2 scores up to internal temperature of −0.70 °C. From −0.7 °C to −0.9 °C the spectra showed a slow decrease of PC2 and PC1scores. This long period between −0.7 and −0.9 °C is related to the reaching of the chemical potential in equilibrium between liquid and solid phases, i.e., the freezing point. Indeed, after that period a fast decrease in PC2 scores, always linked to temperature decrease, was recorded up to −2.0 °C internal temperature. The sample displacement in the scores plot is well explained by the related loadings (Fig. 8b). PC1 loadings assume positive values at 970 and 1160 nm related to water molecule combination of symmetric stretch and bending mode (970 nm), and symmetric stretch, asymmetric stretch and bending mode (1200 nm) when it is liquid but near to the freezing point. Whereas PC1 assumed negative values at 1030 and 1260 nm, which can be related to the water molecule combination of symmetric stretch and bending mode (1025 nm), and symmetric stretch, asymmetric stretch and bending mode (1250 nm) when it is ice.

Due to the relevance of PC1 in describing the phenomena, PC1 scores of all the trials are represented in function of temperature in Fig. 8c.

Strength of the high relation between PC1 scores and phase changes of water contained in the beef cubes, a PCA was calculated for the construction of a multivariate control chart to monitor the SC process. When using a PCA to build a predictive model, and not just as an explorative tool, it is necessary to validate the model to assess its performance in prediction. Thus, trial 1, 2 and 4 were selected for model calibration, whereas trial 3 was remove and, later, used to validate the model.

The Q residual vs T^2 plot built in calibration confirmed that spectra

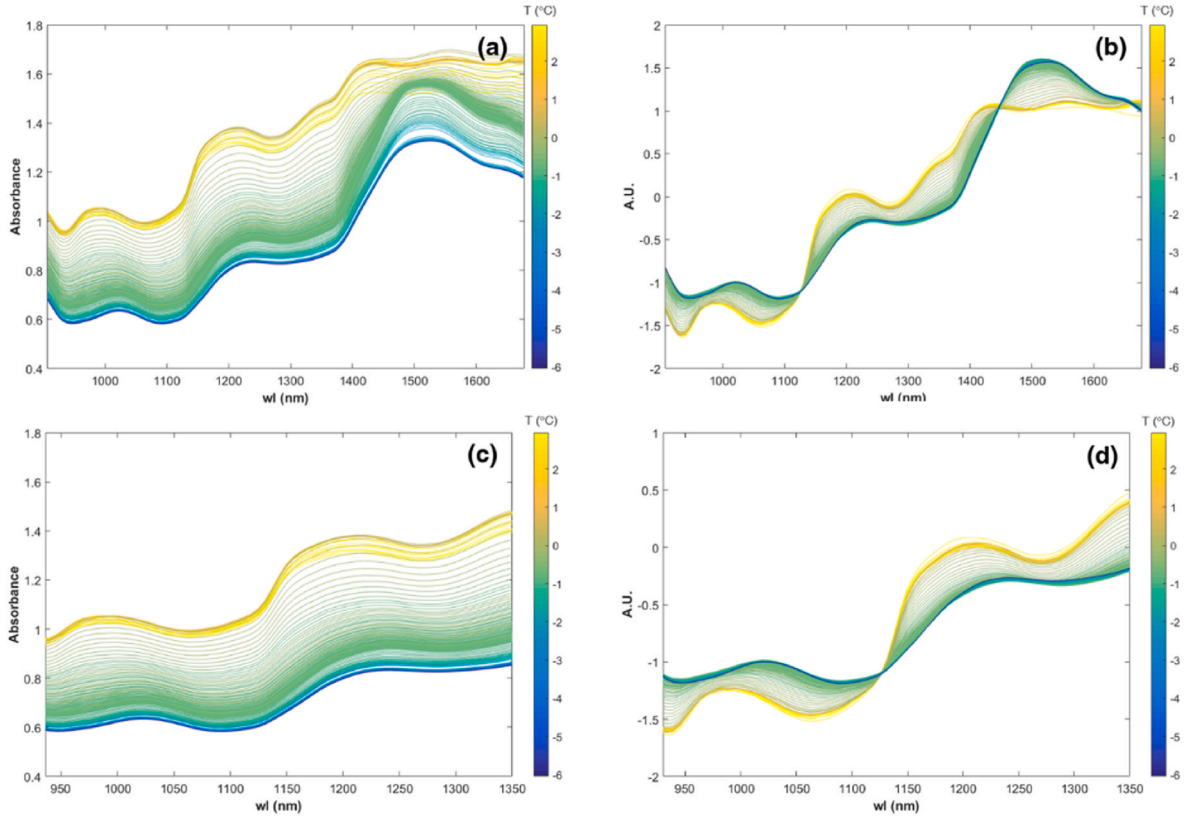

Fig. 7. Spectra recorded along trial 4 coloured according to internal temperature (T, °C) recorded by temperature probe: A) raw spectra in the whole MicroNIR range, B) SNV spectra in the whole MicroNIR range, C) raw spectra in the range 940–1350 nm, D) SNV spectra in the range 940–1350 nm.

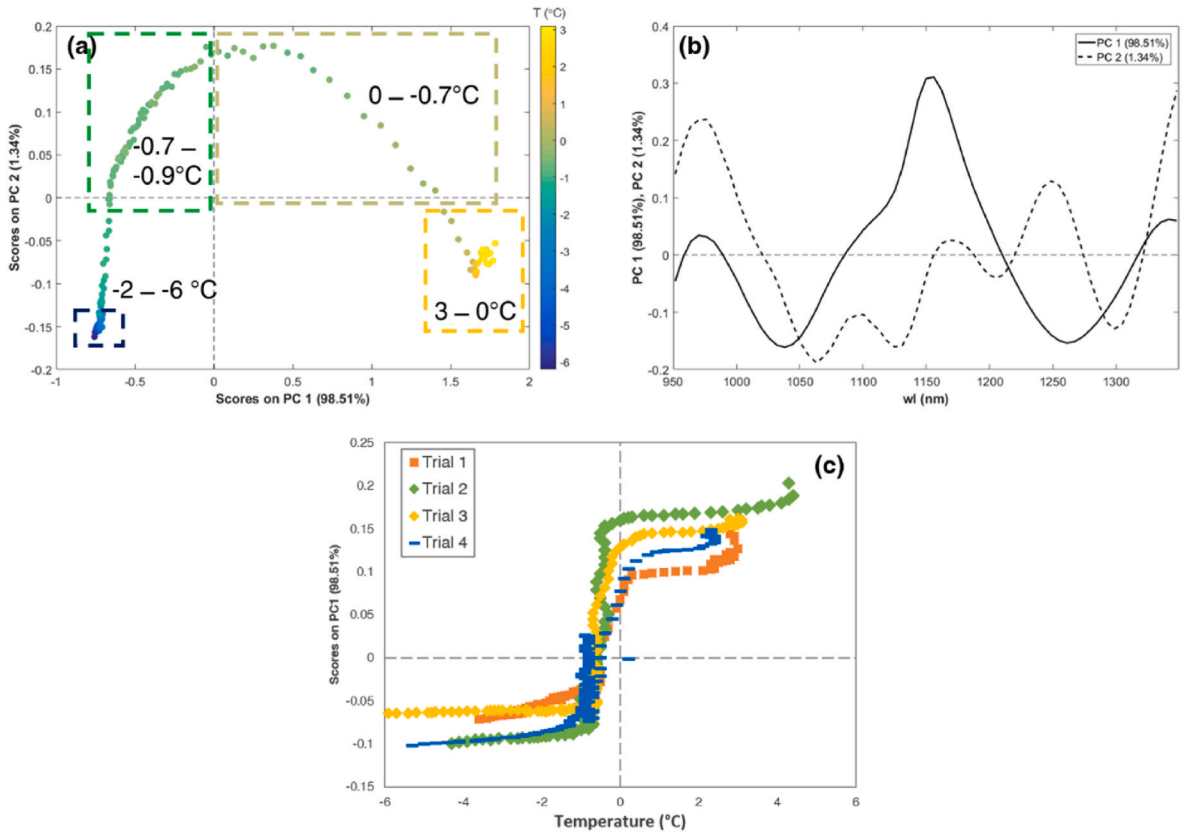

Fig. 8. Principal Component Analysis on the SNV spectra collected for the 4 trials: A) PC1 vs PC2 scores plot of trial 4, B) PC1 and PC2 loadings plot, C) PC1 scores vs internal temperature recorded for all the 4 trials.

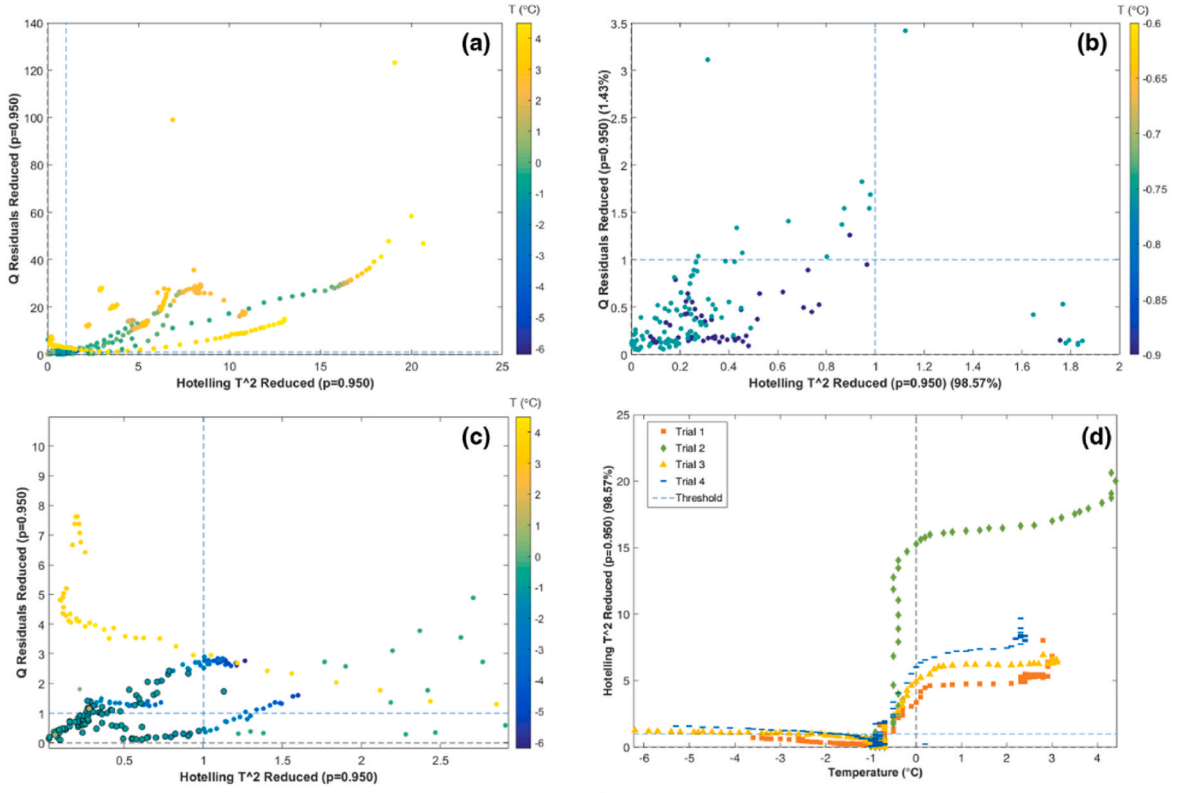

Fig. 9. Multivariate Statistical Process Control (MSPC) based on PCA: A) Q residual vs T2 plot from PCA calibration, B) zoom of Q residual vs T2 plot from PCA calibration, C) projection of external test set on the Q residual vs T2 space, D) T2 vs internal temperature plot with samples coloured according to trials.

recorded when internal temperature were higher than the freezing point assumed high T^2 values, meaning that these points are far from the centre of the PCA model (Fig. 9a). By zooming in the set statistic threshold ($p = 0.95$) (Fig. 9b) it is easiest to notice that the spectra falling within this limit belong to records with internal temperature between −0.75 °C and −0.90 °C. When projecting the prediction test (trial 3) in the Q residual vs T^2 space (Fig. 9c), the spectra recorded around the Tf assumed T^2 values within the statistic threshold ($p = 0.95$), confirming that a control chart based on T^2 could be used to assess the achievement of SC internal condition even from a NIR spectra recorded on the sample surface. By observing the T^2 vs. temperature (Fig. 9d) it is possible to recognise a distribution trend like the one observed for PC1 scores (Fig. 8c). The spectra recorded after the nucleation/in the crystallization phase (liquid water and ice equilibrium) fall within the statistic threshold ($p = 0.95$).

3.4. Practical applications/Potential

The SC storage of meat implies temperatures below its initial freezing point. While the use of these temperatures has undoubtful advantages for extending the shelf life of meat (Pomponio and Ruiz-Carrascal, 2017), it also leads to the formation of a certain proportion of ice (Duun et al., 2008). In turn, this may lead to some deleterious effects on meat quality, such as structural damages, drip loss, lipid oxidation and so on. Therefore, the implementation of potential tools that enable estimating the amount of ice formed during the SC process might allow optimizing SC based not only on the temperature during the process but on the actual amount of ice formed, which is the direct cause of meat quality loss. In fact, the calculation of the proportion of ice as a function of actual sub-zero temperature assumes a steady state in which the temperature is kept for as long as necessary to reach an equilibrium between the water and ice fractions. However, during the period of thermal arrest, while there is almost no variation in temperature, there is a steady increase in the proportion of ice. Therefore, during this period it is not possible to infer such a proportion of solid water based on temperature measurement.

Interestingly, the results obtained in this study point out that both techniques, NIRs and ultrasound inspection, are capable of detecting the dramatically fast ice crystal formation during the period of thermal arrest, during which temperature remains more or less constant. This fact indicates that, these non-destructive analytical techniques might be implemented as quality control tools during the SC process of muscle foods (or even other type of foods), enabling to monitor the ice crystal formation. In turn, this may allow optimizing the amount of ice formed during SC of muscle foods to the desired specific level, minimizing the potential deleterious effects of ice formation in meat.

4. Conclusions

Temperature is usually the only information that meat companies have for monitoring the freezing of meat surface during the SC process. A temperature well below the freezing point of meat for an enough time is directly related to a high proportion of water in frozen form. However, around the freezing temperature of water in meat and for a period of time (the so-called period of thermal arrest), there is an increasing amount of frozen water without a decrease in temperature, making the measured temperature an inadequate predictor of ice crystal formation. Interestingly, both NIR and ultrasound measurements are capable of providing information showing the changes in the amount of frozen water during this period of thermal arrest. This fact makes these two techniques potential useful tools for monitoring the formation of ice during the optimization of the SC process for meat and muscle foods in general.

CRediT authorship contribution statement

Silvia Grassi: Conceptualization, Data curation, Formal analysis, Investigation, Methodology, Software, Supervision, Validation, Visualization, Writing – original draft, Writing – review & editing. **Antonio Jiménez:** Conceptualization, Data curation, Formal analysis, Investigation, Methodology, Software, Supervision, Validation, Visualization, Writing – original draft, Writing – review & editing, Funding acquisition, Project administration, Resources. **Jorge Ruiz:** Conceptualization, Funding acquisition, Investigation, Methodology, Project administration, Resources, Supervision, Validation, Visualization, Writing – original draft, Writing – review & editing. **Alberto González-Mohino:** Conceptualization, Data curation, Formal analysis, Investigation, Methodology, Software, Supervision, Validation, Visualization, Writing – original draft, Writing – review & editing.

Declaration of competing interest

The authors declare that they have no known competing financial interests or personal relationships that could have appeared to influence the work reported in this paper.

Data availability

Data will be made available on request.

References

Abdul Halim, M.H., Buniyamin, N., Mohd Shari, M.A., Abu Kassim, R., 2012. Ultrasound velocity to measure beef, chicken and fish fillet fat content. SCOReD 2012 - 2012 IEEE Student Conf. Res. Dev. 54–58. https://doi.org/10.1109/SCOReD.2012.6518610.

Alamprese, C., Amigo, J.M., Casiraghi, E., Engelsen, S.B., 2016. Identification and quantification of Turkey meat adulteration in fresh, frozen-thawed and cooked minced beef by FT-NIR spectroscopy and chemometrics. Meat Sci. https://doi.org/10.1016/j.meatsci.2016.06.018.

Awad, T.S.S., Moharram, H.A.A., Shaltout, O.E.E., Asker, D., Youssef, M.M.M., 2012. Applications of ultrasound in analysis, processing and quality control of food: a review. Food Res. Int. 48, 410–427. https://doi.org/10.1016/j.foodres.2012.05.004.

Banerjee, R., Maheswarappa, N.B., 2019. Superchilling of muscle foods: potential alternative for chilling and freezing. Crit. Rev. Food Sci. Nutr. 59, 1256–1263. https://doi.org/10.1080/10408398.2017.1401975.

Contreras, M., Benedito, J., Quiles, A., Lorenzo, J.M., Fulladosa, E., Gou, P., Garcia-Perez, J.V., 2020. Assessing the textural defect of pastiness in dry-cured pork ham using chemical, microstructural, textural and ultrasonic analyses. J. Food Eng. 265 https://doi.org/10.1016/j.jfoodeng.2019.109690.

Cruz, C., Fonte, C.P., De Simone, A., Oppong, F.K., Jeatt, W., Rodgers, T.L., 2023. Study of fast in-line measurement techniques for water ice characterization. J. Food Eng. 353, 111550 https://doi.org/10.1016/j.jfoodeng.2023.111550.

de Prados, M., García-Pérez, J.V., Benedito, J., 2015. Non-destructive salt content prediction in brined pork meat using ultrasound technology. J. Food Eng. 154, 39–48. https://doi.org/10.1016/j.jfoodeng.2014.12.024.

Diaz-Almanza, S., García-Galicia, I.A., Rentería-Monterrubio, A.L., Reyes-Villagrana, R. A., 2021. Analysis of the simultaneous measurement of acoustic phase velocity and stress-strain relationship in beef: an approach to Young's modulus. Appl. Acoust. 182, 108237 https://doi.org/10.1016/j.apacoust.2021.108237.

Djekic, I., Tomasevic, I., 2016. Environmental impacts of the meat chain – current status and future perspectives. Trends Food Sci. Technol. 54, 94–102. https://doi.org/10.1016/j.tifs.2016.06.001.

Duun, A.S., Hemmingsen, A.K.T., Haugland, A., Rustad, T., 2008. Quality changes during superchilled storage of pork roast. LWT–Food Sci. Technol. 41, 2136–2143. https://doi.org/10.1016/j.lwt.2008.02.001.

Ensminger, D., Bond, L.J., 2011. Ultrasonics: Fundamentals, Technologies, and Applications. CRC press.

Fariñas, L., Contreras, M., Sanchez-Jimenez, V., Benedito, J., Garcia-Perez, J.V., 2021. Use of air-coupled ultrasound for the non-invasive characterization of the textural properties of pork burger patties. J. Food Eng. 297, 110481 https://doi.org/10.1016/j.jfoodeng.2021.110481.

González-Mohino, A., Jiménez, A., Paniagua, M.J., Perez-Palacios, T., Rufo, M., 2019a. New contributions of ultrasound inspection to the characterization of different varieties of honey. Ultrasonics. https://doi.org/10.1016/j.ultras.2019.02.010.

González-Mohino, A., Jiménez, A., Rufo, M., Paniagua, J.M., Antequera, T., Perez-Palacios, T., 2022. Ultrasound parameters used to characterize Iberian fresh pork loins of different feeding systems. J. Food Eng. 314, 110795 https://doi.org/10.1016/j.jfoodeng.2021.110795.

González-Mohino, A., Jiménez, A., Rufo, M., Paniagua, J.M., Nas, S.V., Olegario, L.S., 2019b. Changes of ultrasonic parameters as a tool to determine the influence of cooking in pork loin samples. Acta Acust. united with Acust. 105, 943–952.
Gowen, A.A., Amigo, J.M., Tsenkova, R., 2013. Characterisation of hydrogen bond perturbations in aqueous systems using aquaphotomics and multivariate curve resolution-alternating least squares. Anal. Chim. Acta 759, 8–20.
Grassi, S., Casiraghi, E., Alamprese, C., 2018. Handheld NIR device: a non-targeted approach to assess authenticity of fish fillets and patties. Food Chem. 243, 382–388. https://doi.org/10.1016/j.foodchem.2017.09.145.
Gudra, T., Opielinski, K.J., 2004. Applying spectrum analysis and cepstrum analysis to examine the cavitation threshold in water and in salt solution. Ultrasonics 42, 621–627. https://doi.org/10.1016/j.ultras.2003.11.016.
Jiménez, A., Rufo, M., Paniagua, J., González-Mohino, A., Olegario, L.S., 2022. New findings of edible oil characterization by ultrasonic parameters. Food Chem. 374, 131721 https://doi.org/10.1016/j.foodchem.2021.131721.
Kademi, H.I., Ulusoy, B.H., Hecer, C., 2019. Applications of miniaturized and portable near infrared spectroscopy (NIRS) for inspection and control of meat and meat products. Food Rev. Int. 35, 201–220.
Kinsler, L.E., Frey, A.R., Coppens, A.B., Sanders, J.V., 1999. Fundamentals of acoustics. Fundam. Acoust. In: Lawrence E. Kinsler, Austin R. Frey, Alan B. Coppens, fourth ed. James V. Sanders, p. 560. https://doi.org/10.1002/9780470612439. 0-471-84789-5. Wiley-VCH, December 1999.
MacGregor, J.F., Kourti, T., 1995. Statistical process control of multivariate processes. Control Eng. Pract. 3, 403–414. https://doi.org/10.1016/0967-0661(95)00014-L.
Niñoles, L., Mulet, A., Ventanas, S., Benedito, J., 2011. Ultrasonic characterisation of B. femoris from Iberian pigs of different genetics and feeding systems. Meat Sci. 89, 174–180. https://doi.org/10.1016/j.meatsci.2011.04.014.
Nowak, K.W., Markowski, M., 2013. A comparison of methods for the determination of sound velocity in biological materials: a case study. Ultrasonics 53, 923–927. https://doi.org/10.1016/j.ultras.2013.01.009.
Ottestad, S., Høy, M., Stevik, A., Wold, J.P., 2009. Prediction of ice fraction and fat content in super-chilled salmon by non-contact interactance near infrared imaging. J. Near Infrared Spectrosc. 17 (2), 77–87. https://doi.org/10.1255/jnirs.827.
Pomponio, L., Bukh, C., Ruiz-Carrascal, J., 2018. Proteolysis in pork loins during superchilling and regular chilling storage. Meat Sci. 141, 57–65. https://doi.org/10.1016/j.meatsci.2018.03.022.
Pomponio, L., Ruiz-Carrascal, J., 2017. Oxidative deterioration of pork during superchilling storage. J. Sci. Food Agric. 97, 5211–5215. https://doi.org/10.1002/jsfa.8403.
Rahman, M.S., 2009. Food Properties Handbook. CRC press.
Sanchez, P.D.C., Arogancia, H.B.T., Boyles, K.M., Pontillo, A.J.B., Ali, M.M., 2022. Emerging nondestructive techniques for the quality and safety evaluation of pork and beef: recent advances, challenges, and future perspectives. Appl. Food Res. 2, 100147 https://doi.org/10.1016/j.afres.2022.100147.
Schmerr, L., Song, J.-S., 2007. Ultrasonic Nondestructive Evaluation Systems.
Sigfusson, H., Ziegler, G.R., Coupland, J.N., 2004. Ultrasonic monitoring of food freezing. J. Food Eng. 62, 263–269. https://doi.org/10.1016/S0260-8774(03)00239-5.
Stevik, A.M., Duun, A.S., Rustad, T., O'Farrell, M., Schulerud, H., Ottestad, S., 2010. Ice fraction assessment by near-infrared spectroscopy enhancing automated superchilling process lines. J. Food Eng. 100, 169–177.
Wold, S., Esbensen, K., Geladi, P., 1987. Principal component analysis. Chemometr. Intell. Lab. Syst. 2, 37–52. https://doi.org/10.1016/0169-7439(87)80084-9.
Workman, J., Weyer, I., 2008. Practical Guide to Interpretive Near-Infrared Spectroscopy. CRC Press, Boca Raton.
Xie, A., Sun, D.W., Zhu, Z., Pu, H., 2016. Nondestructive measurements of freezing parameters of frozen porcine meat by NIR hyperspectral imaging. Food. Bioprocess. Technol. 9, 1444–1454. https://doi.org/10.1007/s11947-016-1766-2.